UNIVERSITY OF PARDUBICE

Faculty of Chemical Technology

Department of General and Inorganic Chemistry

Reactivity of *NCN* chelated pnictinidines: ligands for transition metals vs hidden heterodienes

Annotation of Doctoral Thesis

2020

Author: Ing. Monika Kořenková

Supervisor: doc. Ing. Libor Dostál, Ph.D.

The Doctoral Thesis was done at the Department of General and Inorganic Chemistry of University of Pardubice in the Czech Republic during years 2015-2020.

Candidate: Ing. Monika Kořenková

Reviewers: prof. Ing. Antonín Lyčka, DrSc.

doc. Mgr. Pavel Štarha, Ph.D.

prof. RNDr. Jiří Příhoda, CSc.

The Doctoral Thesis will be available in the Library of University of Pardubice.

1. INTRODUCTION

The chemistry of monomeric organometallic compounds R–E (where E = P, As, Sb or Bi) containing pnictogen central atom in the oxidation state +*I* (i.e. pnictinidenes) offers various bonding situation often corresponding to different variants of their structure interpretation. While the chemistry of phosphorus is quite rich[1], the number of isolated derivatives decreases steeply with increasing proton number of the central atom. The electron configuration of the pnictogen suggests that there are two lone electron pairs on the central atom that can be used for donation and subsequent complex formation with transition metals (TM).[2] Until recently, however, this area has been sparsely studied because of the high reactivity and difficulty of isolating heavier pnictinidenes.

Previous works have shown,[3] that heavier pnictinidenes prefer the formation of 1:1 complexes and, in this regard, carbonyl complexes were studied. Only a few cases are known where the heavier pnictinidene forms a bridge between two TMs and, thus, acts as a four-electron donor. These examples include the complexes in the Figure 1.[4,5] Based on these results, a study of reactivity of ArE [Ar = C_6H_3-2,6-(CH=N*t*Bu)$_2$, E = Sb or Bi] to selected late TM complexes was conducted to prove their potential to coordinate other than carbonyl complexes at all and to examine the possibility to serve as four-electron donors.

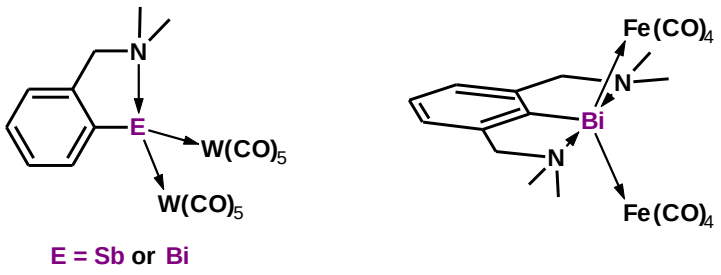

Figure 1 Pnictinidene as a four-electron donor bridging two TMs.

Another interesting feature of the low-valent compounds of the pnictogens, especially the phosphorus and arsenic derivatives, is their noticeable heterocyclic character when particular *(N)CN* chelating ligand is used (Scheme 1).[6] It is logical to expect this bonding situation to be substantially suppressed for heavier analogs but has never been experimentally ruled out. Thus, a study of the reactivity of ArE [Ar = C_6H_3-

2,6-(CH=N*t*Bu)$_2$, E = Sb or Bi] to selected strong dienophiles was also conducted to determine whether the discussed pnictinidenes are capable of addition to multiple C=C and C≡C bonds. These Diels-Alder reactions, which contain a nitrogen atom in heterocyclic products, are relatively well known.[7] However, in the case of heavier pnictogens, this area is less well studied. Only recently, a heterocycle containing Bi atom prepared from bismabenzene using RC≡CR, where R = CO_2Me (DMAD), was published.[8]

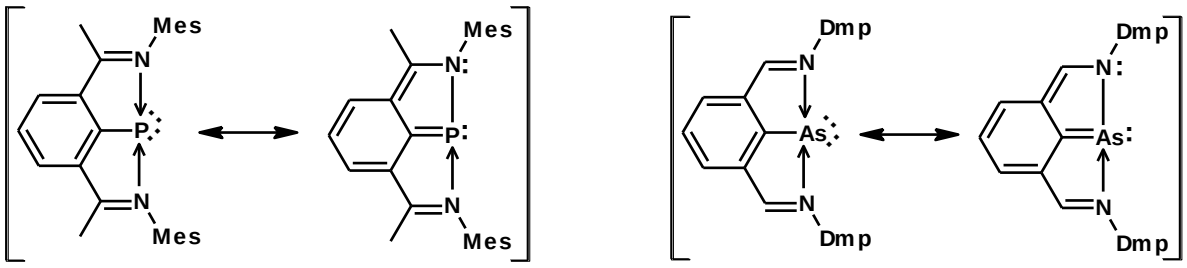

Scheme 1 Resonance structures of NCN chelated phosphinidene and arsinidene.

2. RESULTS AND DISCUSSION

2.1. Coordination studies of pnictinidenes ArE (E = Sb or Bi)

Group 9 complexes

Compound ArSb was reacted with the dimeric complex [(cod)M(μ-Cl)]$_2$, where cod = 1,5-cyclooctadiene, M = Rh or Ir, in toluene at room temperature and within 5 minutes the desired complexes [ArSbM(Cl)(cod)] [**1** (M = Ir) or **2** (M = Rh)] were formed (Scheme 2).

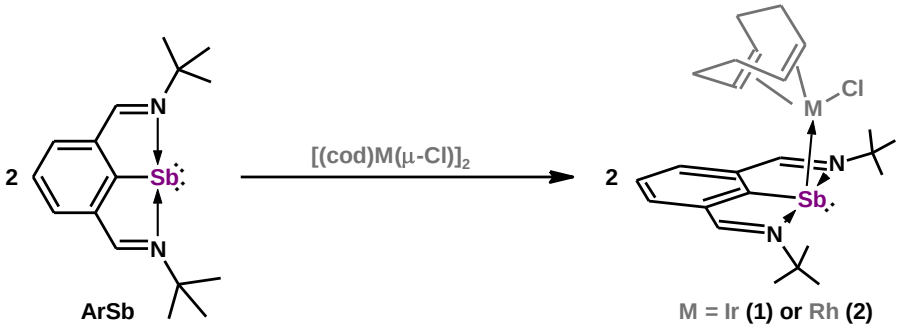

*Scheme 2 The synthesis of compounds **1** and **2**.*

Characterization in solution was performed using ^{1}H a ^{13}C{^{1}H} NMR spectroscopy in C_6D_6. Both spectra contain one set of sharp signals corresponding to the pincer ligand

for compound **1** and **2**, including one typical singlet for *CH*=N group with $\delta(^1H)$ = 8.41 and 8.50 ppm and $\delta(^{13}C)$ = 157.4 and 156.7 ppm and one singlet for $(CH_3)_3C$ group with $\delta(^1H)$ = 1.54 and 1.65 ppm and $\delta(^{13}C)$ = 32.7 and 33.0 ppm. A typical set of signals was also detected for cod ligand. In the ^1H and $^{13}C\{^1H\}$ NMR spectra, two signals with $\delta(^1H)$ = 1.88 and 5.02 ppm for **1** and 1.91 and 5.50 ppm for **2** [$\delta(^{13}C)$ = 51.4 and 78.9 ppm for **1** and 67.8 and 94.4 ppm for **2**] were observed for the *CH*-cod groups. In the case of $^{13}C\{^1H\}$ NMR spectrum of compound **2**, both signals are cleaved into doublets due to the presence of a rhodium atom (100% representation of ^{103}Rh, I = ½) with *J*-coupling constant of $^1J_{RhC}$ = 14.0 and 9.0 Hz. For the *CH₂*-cod groups, four signals with chemical shifts in range of 1.11 – 1.94 ppm for **1** and 1.36 – 2.08 ppm for **2** are detected in the ^1H NMR spectrum, while two signals remain in the $^{13}C\{^1H\}$ NMR spectrum with chemical shifts of 30.4 and 35.2 ppm for **1** and 29.5 and 34.4 ppm for **2**.

The molecular structure of **2** was unambiguously confirmed by X-ray analysis (Figure 2). The Sb atom is tightly coordinated in the cavity of pincer ligand, which corresponds to the C1–Sb covalent bond 2.092(3) Å, and is further stabilized by the presence of strong intramolecular N→Sb interactions characterized by 2.423(2) and 2.348(2) Å bond lengths. These values are close to the sum of the covalent radii Σ_{cov}(N–Sb) = 2.11 Å and are significantly shorter than Σ_{vdW}(Sb–N) = 3.74 Å. Bond angle N1–Sb–N2 146.18(8)° corresponds to the pseudo-meridional coordination of the pincer ligand. As expected,[3] the rhodium atom is coordinated almost perpendicularly to the plane of the ArSb ligand with the bond angle C1–Sb1–Rh1 being 107.30(5)°. This phenomenon appears due to the use of *p*-type electron pair of the antimony for the formation of dative bond with vacant orbital of rhodium. The deviation from hypothetical right angle may be caused by steric reasons. There is a slightly deformed square-planar arrangement on the Rh central atom with bond length of Sb–Rh being 2.6511(3) Å which corresponds to Σ_{cov}(Rh–Sb) = 2.65 Å.

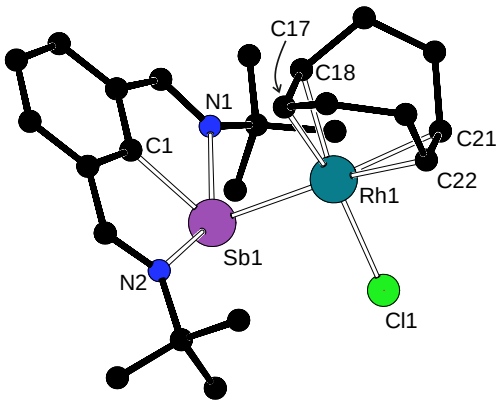

*Figure 2 Molecular structure of compound **2**.*

Reaction of stibinidene ArSb with an analogous dimeric complex $[(cot)_2Rh(\mu\text{-}Cl)]_2$, where cot = cyclooctene, produced an insoluble black precipitate at room temperature after 5 minutes (Scheme 3). After evaporation of the mixture and subsequent benzene extraction, compound **3** could be isolated as a result of transmetallation.

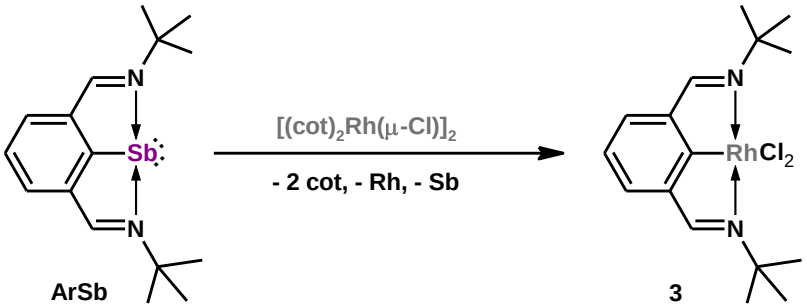

*Scheme 3 The synthesis of compound **3**.*

Characterization of compound **3** in solution was performed using ^{1}H a $^{13}C\{^{1}H\}$ NMR spectroscopy in C_6D_6. One set of sharp signals that corresponds to the pincer ligand was observed. The signal for *CH*=N groups is found at $\delta(^{1}H)$ = 7.55 ppm and $\delta(^{13}C)$ = 167.6 ppm. In the case of ^{1}H NMR spectrum, this signal is cleaved to doublet due to the spin-spin interaction with Rh atom with $^{n}J_{RhH}$ = 3.9 Hz. Similarly, the signal of *ipso*-carbon in $^{13}C\{^{1}H\}$ NMR spectrum occurs as a doublet with $\delta(^{13}C)$ = 184.0 ppm and $^{1}J_{RhC}$ = 30.2 Hz.

Molecular structure of **3** could be confirmed by X-ray analysis (Figure 3). The central Rh atom is again tightly coordinated by the pincer ligand in a tridentate pseudo-

meridional fashion with a bond angle N1–Rh–N2 being 161.87(9)°. Rh–N bond lengths of 2.052(2) and 2.053 (2) Å correspond to Σ_{cov}(Rh–N) = 1.96 Å.

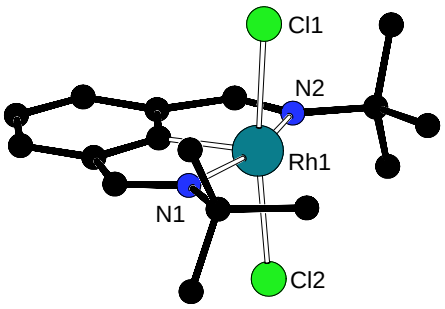

*Figure 3 Molecular structure of compound **3**.*

Group 10 complexes

Stibinidene ArSb was reacted with one equivalent of [$PtCl_2L_2$], where L = Me_2S or dmso, in thf at room temperature and after 30 minutes the precipitated 1:1 *cis*-[$PtCl_2L(ArSb)$] complexes [**4** (L = Me_2S) and **5** (L = dmso)] were isolated (Scheme 4).

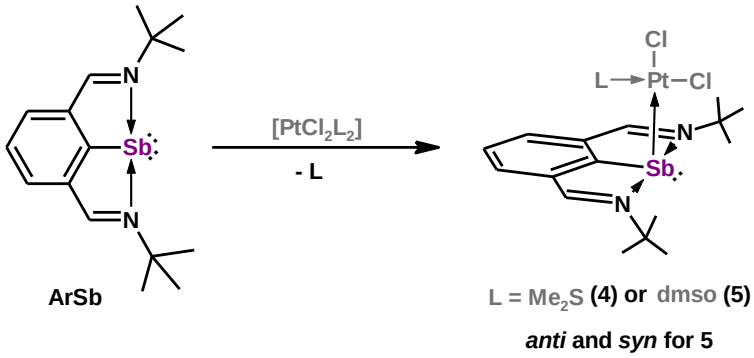

*Scheme 4 The synthesis of compounds **4** and **5**.*

Structure in solution was determined by ^{1}H a ^{13}C{^{1}H} NMR spectroscopy in $CDCl_3$. The spectra of compound **4** contain one set of signals for pincer ligand with a typical chemical shift for *CH*=N groups with δ(^{1}H) = 8.86 ppm and δ(^{13}C) = 159.3 ppm. The proposed structure is further confirmed by a typical singlet for Me_2S ligand with δ(^{1}H) = 2.06 ppm and δ(^{13}C) = 23.5 ppm, whereas satellites due to interaction with ^{195}Pt ($^3J_{PtH}$ = 53.4 Hz) can be observed in ^{1}H NMR spectrum. In case of compound **5**, however, the situation is more complicated. The NMR spectra contain two sets of signals in a integral ratio of 1:0.9, which are caused by the formation of two rotamers, whose existence was

caused by a limited rotation around the dative Sb→Pt bond and at the same time by preferential orientation of ArSb ligand towards dmso ligand. If the aromatic ring of the ArSb ligand is oriented to the chlorine atom on the Pt atom, it is an *anti*-**5** rotamer (which was also characterized in the solid phase by X-ray analysis, see below). In the second case, when the aromatic ring of the ArSb ligand is oriented to the dmso ligand, we can refer to the *syn*-**5** rotamer (Figure 4). Compound **4** does not produce rotamers probably due to the less bulky Me_2S ligand, which does not prevent free rotation around the Sb–Pt bond in terms of the NMR time scale.

The above phenomenon is manifested in the NMR spectra by, for example, the signal of *CH*=N groups in compound **5** confirming the presence of the pincer ligand which occurs with $\delta(^1H)$ = 8.87 and 8.77 ppm and $\delta(^{13}C)$ = 160.1 and 160.7 ppm for *anti*/*syn*-**5**. Methyl groups of dmso ligand of a given rotamer are equivalent in both rotamers, providing a singlet with $\delta(^1H)$ = 3.03 and 3.66 ppm for *anti*/*syn*-**5** and $\delta(^{13}C)$ = 46.8 ppm, which corresponds to the overlap signals of both rotamers.

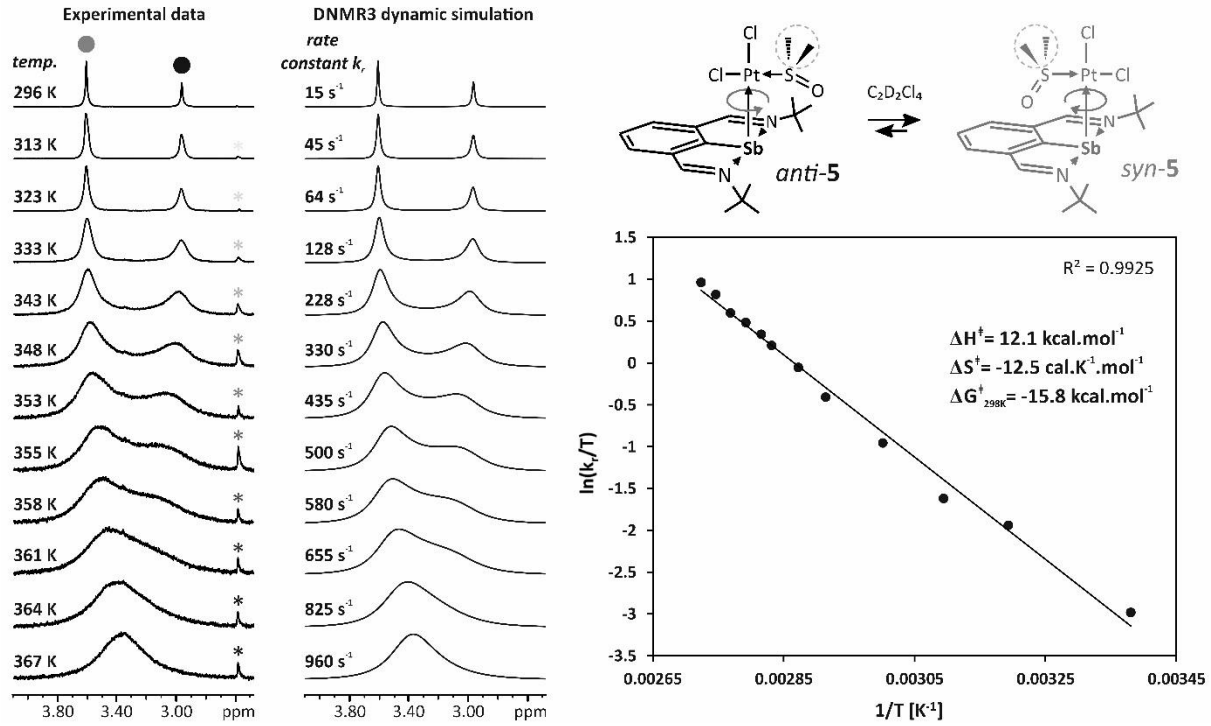

*Figure 4 Stacked plot of ^1H VT-NMR spectroscopy (400.13 MHz, $C_2D_2Cl_4$) showing the Me groups region of dmso of compound **5**, dynamic NMR simulation of experimental data and Eyring plot. * indicates a traces of impurities.*

The nature of this dynamic process was also studied by ^1H VT-NMR spectroscopy (Figure 4). However, it was not possible to achieve coalescence of signals in $CDCl_3$ due to

the temperature limit of the solvent given by its low boiling point. Indeed, by increasing the sample temperature in high-boiling $C_2D_2Cl_4$, the signals broadened and eventually coalesced. This process is reversible. The rate constants k_r were obtained from the experimental data with help of DNMR3 simulation (based on mathematical analysis of the signals shape), of which dependence on 1/T were thermodynamic activation parameters calculated by substituting into the Eyring equation: $\Delta G^{\ddagger}_{298K}$ = 15.8 kcal·mol^{-1}; $\Delta H^{\ddagger}$ = 12.1 kcal·mol^{-1} and $\Delta S^{\ddagger}$ = −12.5 cal·K^{-1}·mol^{-1}.

The molecular structures of compounds **4** and *anti*-**5** could be confirmed by X-ray analysis (Figure 5). The bonding arrangement within the ArSb ligand is analogous to the previous cases. Thus, the Sb atom is found in the pincer ligand cavity with intramolecular interactions of N→Sb [2.378(3) and 2.479(4) Å for **4**; 2.425(7) and 2.399(7) Å for *anti*-**5**]. The central Pt atom is found in a square-planar surroundings with *cis*-orientation of Cl atoms. The Pt–Sb bond lengths of 2.5432(5) and 2.5694(7) Å in **4** and *anti*-**5** are shorter compared to Σ_{cov}(Sb–Pt) = 2.63 Å. The ArSb ligand is again coordinated almost perpendicularly, with the C1-Sb1-Pt1 bond angle of 103.98(14)° for **4** and 106.0(2)° for *anti*-**5**.

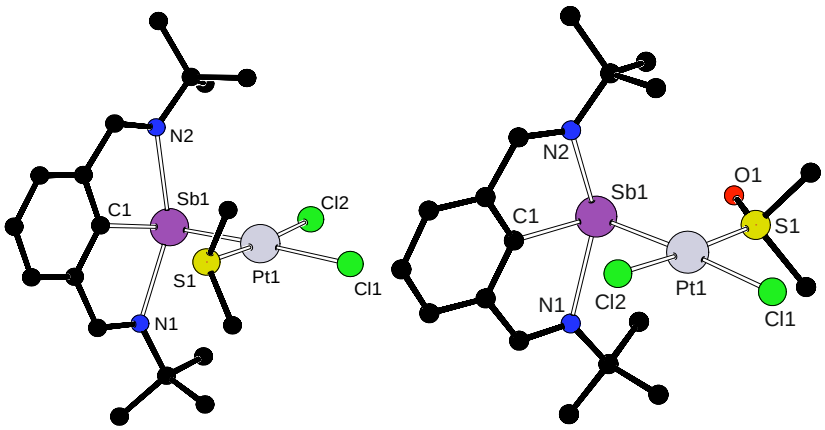

*Figure 5 Molecular structures of compounds **4** (left) and anti-**5** (right).*

An effort to prepare analogous palladium complexes was not successful. Elemental palladium was formed immediately due to high redox reactivity of ArSb. In order to increase the stability of the resulting complexes, attention was paid to complexes containing another stabilizing *CN* chelating ligand. Reaction of ArSb with [RPd(μ-Cl)]$_2$ and [RPtCl(dmso)], where R = C_6H_4-2-(CH_2NMe_2), in thf at room

temperature gave after 5 minutes the expected complexes [RMCl(ArSb)] [**6** (M = Pd) and **7** (M = Pt)] (Scheme 5).

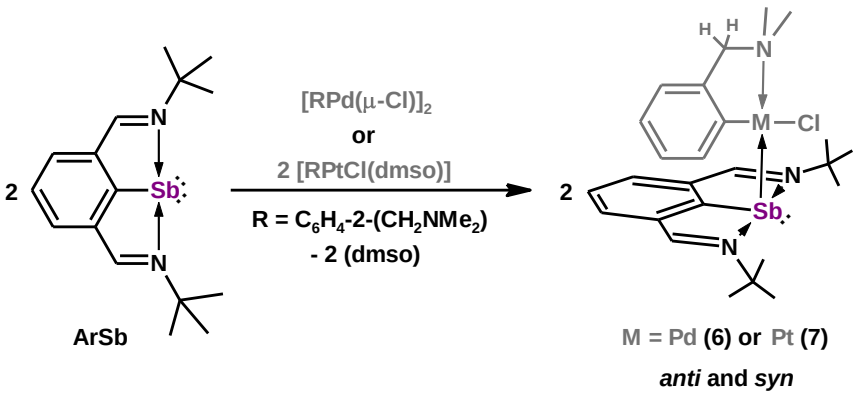

*Scheme 5 The synthesis of compounds **6** and **7**.*

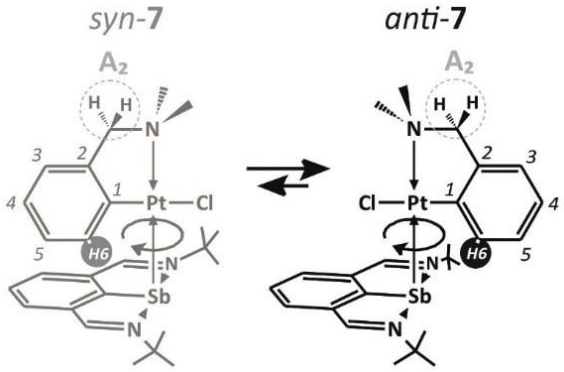

*Scheme 6 Comparison of syn- and anti-rotamers of compound **7**.*

^{1}H a ^{13}C{^{1}H} NMR spectra of compounds **6** and **7** were measured in $CDCl_3$ and they contain two sets of signals in an integral ratio of 1:0.5 for **6** and 1:0.2 for **7,** again, due to the formation of two rotamers in both cases (Scheme 6). The signals of the *CH*=N group characteristic for the ArSb ligand are observed with chemical shifts in the interval of δ(^{1}H) = 8.78 – 8.88 ppm and δ(^{13}C) = 157.8 – 159.3 ppm. The *CN* chelate revealed typical singlet for (CH_3)$_2$N moities in the interval of δ(^{1}H) = 2.61 – 2.92 ppm and δ(^{13}C) = 49.7 – 50.6 ppm; and a singlet for CH_2N as A_2 spin system found at δ(^{1}H) = 3.81 – 3.73 ppm and δ(^{13}C) = 72.3 – 73.9 ppm.

It has been shown that each set of signals can be definitely assigned to a particular rotamer. As a result of the *syn*-rotamer rotation, the *H*6 proton of the *CN* chelate is influenced by the anisotropic effect of the aromatic ring of ArSb ligand (Scheme 6). Thus, this proton is significantly shifted to a higher field [compare δ(^{1}H) =

8.25 ppm for *anti*-**6** vs 5.46 ppm for *syn*-**6** or δ(^{1}H) = 8.31 ppm ($^3J_{PtH}$ = 68.2 Hz) for *anti*-**7** vs 5.66 ppm ($^3J_{PtH}$ = 53.0 Hz) for *syn*-**7**].

Similar products are formed by the reaction of ArSb with ferrocenyl-substituted *CN* chelates of palladium and platinum [RPd(μ-Cl)]$_2$ or [RPtCl(dmso)], where R = Fe[η^5-C$_5$H$_5$][η^5-C$_5$H$_3$-2-(CH$_2$NMe$_2$)] in toluene at room temperature. After work-up, the corresponding complexes [RMCl(ArSb)] [**8** (M = Pd) and **9** (M = Pt)] were isolated (Scheme 7).

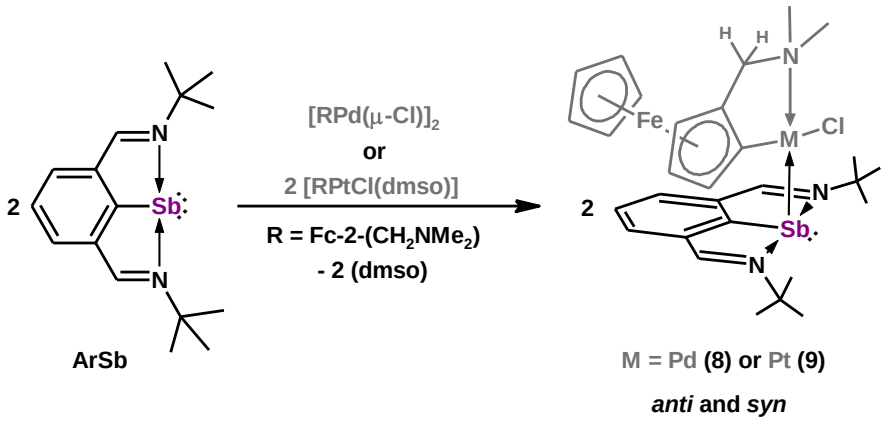

*Scheme 7 The synthesis of compounds **8** and **9**.*

Compounds **8** and **9** also form rotamers in solution (Scheme 8) and contain two sets of signals in the ^{1}H and ^{13}C(^{1}H) NMR spectra, which are more complex due to the presence of planar-chiral ferrocenyl fragment. Thus, the *CH*=N groups of the pincer ligand of both rotamers are not equivalent to each other and even four singlets can be observed with δ(^{1}H) = 8.64 – 9.00 ppm for both *anti*/*syn*-**8** and *anti*/*syn*-**9**; and δ(^{13}C) = 157.5 – 160.5 ppm for both *anti*/*syn*-**8** and *anti*/*syn*-**9**. The (*CH*$_3$)$_2$N groups are also represented by four singlets for both compounds found at δ(^{1}H) = 2.61 – 3.22 ppm; δ(^{13}C) = 50.0 – 52.8 ppm. Signals of *CH*$_2$N group are part of an AX or AB spin system with δ(^{1}H) = 3.15/3.16 and 3.32/3.33 ppm (AB spin system, $^2J_{HH}$ = 14.6/14.2 Hz) for *anti*-**8**/**9**; δ(^{1}H) = 2.95/2.99 and 3.64/3.60 ppm (AX spin system, $^2J_{HH}$ = 13.7 Hz) for *syn*-**8**/**9**. Two signals of this group are also observed in ^{13}C(^{1}H) NMR spectra with δ(^{13}C) = 64.2 – 66.8 ppm for both *anti*/*syn*-**8** and *anti*/*syn*-**9**.

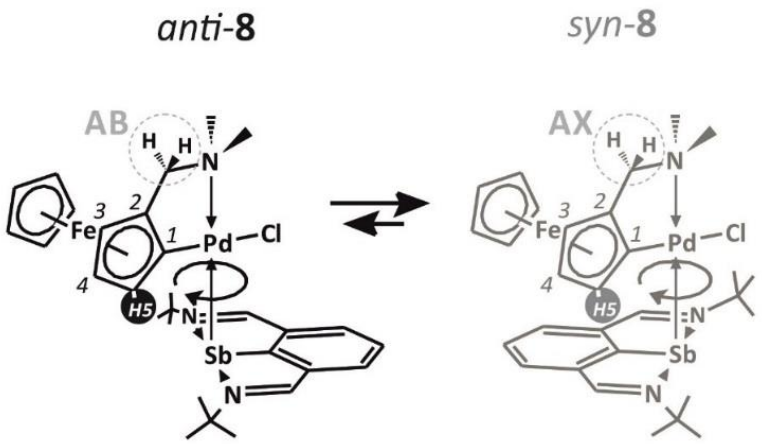

Scheme 8 Comparison of syn- and anti-rotamers of compound **8**.

Analogously to compounds *syn*-**6** and *syn*-**7**, the Cp´ ring of ferrocenyl moiety in compounds *syn*-**8** and *syn*-**9** is also affected by the anisotropic effect of ArSb aromatic ring (Scheme 8). The Cp´-*H*5 protons located above the aromatic ring of the ligand are significantly shifted to higher fields [$\delta(^1H)$ = 4.60 ppm for *anti*-**8** vs 2.00 ppm for *syn*-**8**; $\delta(^1H)$ = 4.54 ppm for *anti*-**9** vs 2.02 ppm for *syn*-**9**].

The molecular structures of compounds **6** – **9** could be confirmed by X-ray analysis (Figure 6). Compounds **6** and **7** contain two independent molecules in the elemental cell, which are structurally very related (and therefore it is not the presence of both rotamers). Side coordination of the ArSb ligand in compounds **6** – **9** is reflected in C1–Sb1–M1 (M1 = Pt1 or Pd1) bond angles ranging from 103.21(17)° to 116.1(3)°. The aromatic ring of ArSb ligand is oriented towards the Cl1 atom in the *anti*-**6** and *anti*-**7** structure, while in *syn*-**8** and *syn*-**9** it is oriented towards the ferrocenyl moiety. The Sb atom is again found in the cavity of the pincer ligand with intramolecular N→Sb interactions in the range of 2.330(10) – 2.465(9) Å. In addition, Sb atom is located in the *trans* position to the N3 atom in all compounds, and the bond angles Sb1–M1–N3 (M1 = Pt1 or Pd1) range from 166.26(14) to 176.9(2)°.

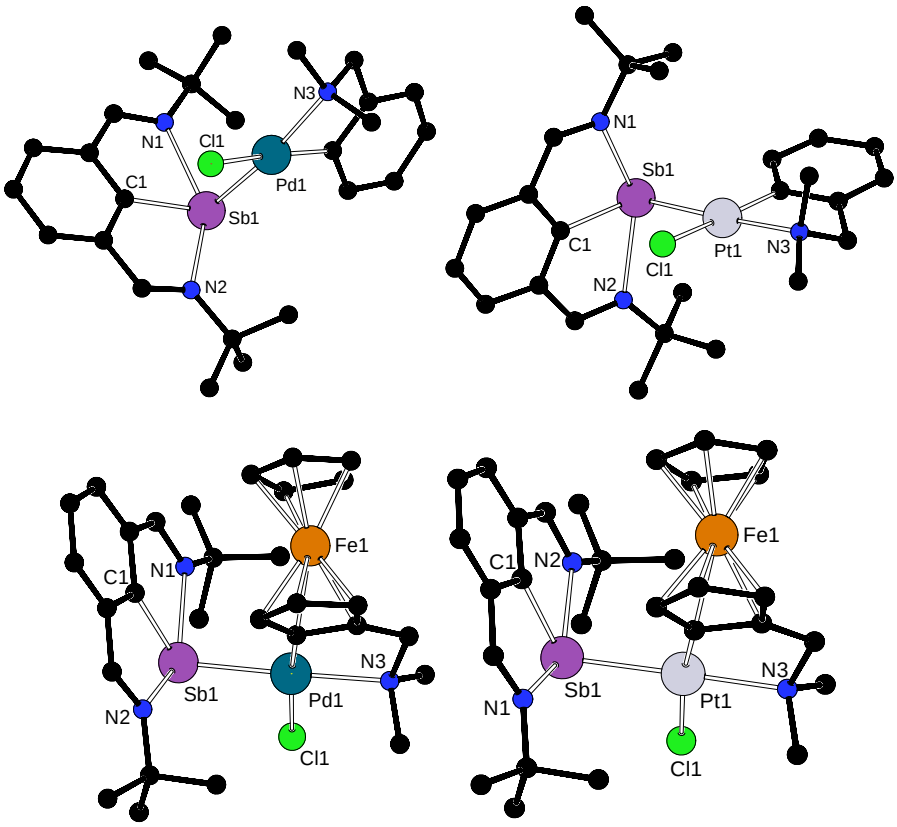

*Figure 6 Molecular structures of compounds anti-**6** (top left), anti-**7** (top right), syn-**8** (bottom left) and syn-**9** (bottom right).*

Palladium (*anti*-**6** and *syn*-**8**) and platinum (*anti*-**7** and *syn*-**9**) atoms are part of the rigid *CN* chelate ring within the expected square-planar arrangement. Bond lengths Pd1–N3 {2.180(5) Å [2.172(5) Å for the second independent molecule] in *anti*-**6** and 2.207(8) Å in *syn*-**8**} and Pt1–N3 {2.153(5) Å [2.150(5) Å for the second independent molecule] in *anti*-**7** and 2.173(9) Å in *syn*-**9**} approach Σ_{cov}(N–M) = 1.91 Å (M = Pd) and 1.94 Å (M = Pt), suggesting strong intramolecular interactions. Bond length Sb1–Pd1 of 2.5363(6) Å [2.5227(6) Å for the second independent molecule] in *anti*-**6** and 2.541(4) Å in *syn*-**8** are significantly shorter than Σ_{cov}(Sb–Pd) = 2.60 Å. Similarly, the bond lengths Sb1–Pt1 of 2.5179(6) Å [2.5291(6) Å for the second independent molecule] in *anti*-**7** and 2.5346(7) Å in *syn*-**9** are shorter than Σ_{cov}(Sb–Pt) = 2.63 Å, but are comparable to those for compounds **4** and *anti*-**5**.

As mentioned in the introduction, there are only a few known cases where heavier pnictinidene forms a bridge between two TMs. Thus, stibinidene ArSb was reacted with one equivalent of the dimer complex $[Pd(\eta^3\text{-}C_3H_5)(\mu\text{-}Cl)]_2$ in thf at room

temperature which quite surprisingly lead to the complex [(Pd(η³-C₃H₅)(Cl)₂(μ-ArSb)] (**10**) (Scheme 9). Therefore, the desired complex was formed in 1:2 ratio.

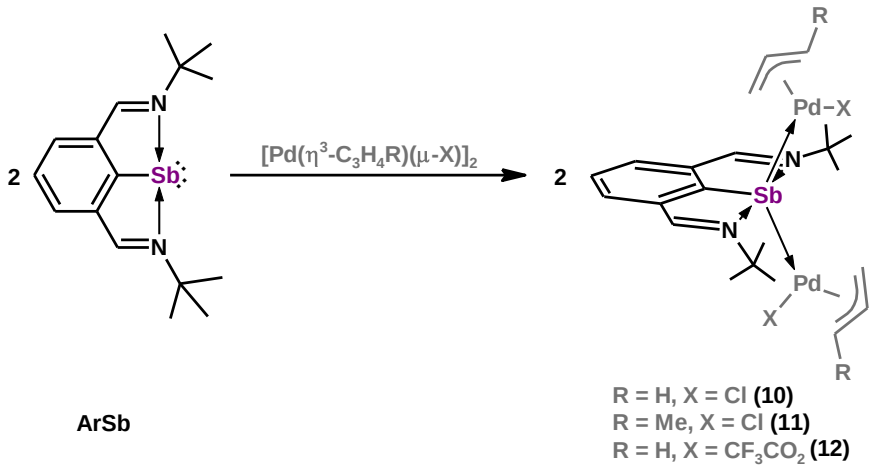

*Scheme 9 The synthesis of compounds **10** – **12**.*

To demonstrate a general nature of this procedure, reactions with [Pd(η³-C₃H₄Me)(μ-Cl)]₂ and [Pd(η³-C₃H₅)(μ-CF₃CO₂)]₂ were carried out to give analogous compounds **11** and **12** (Scheme 9). They are stable as solids in an inert atmosphere for months, but decompose in solution (especially when heated) to form elemental palladium.

The possibility to prepare 1:1 complex was also studied, and indeed it was possible to prepare the expected complex [Pd(η³-C₃H₅)(Cl)(ArSb)] (**13**) by reacting the already prepared complex **10** with another equivalent of stibinidene (Scheme 10). As with the previous complexes, it exhibits only limited stability in solution, but is stable in the solid state.

*Scheme 10 The synthesis of compound **13**.*

All compounds were characterized by ^{1}H a $^{13}C\{^{1}H\}$ NMR spectroscopy in CD_3CN. The spectra of compounds **10** – **12** contain expected signals for the pincer ligand with typical singlets for *CH*=N groups within a narrow range of $\delta(^{1}H)$ = 8.98 – 9.10 ppm and $\delta(^{13}C)$ = 160.0 – 161.9 ppm. For compound **12**, two quartets were found for the CF_3CO_2 group with $\delta(^{13}C)$ = 118.2 ($^{1}J_{CF}$ = 295.4 Hz) for CF_3 and 160.7 ppm ($^{2}J_{CF}$ = 33.0 Hz) for CO_2 in the $^{13}C\{^{1}H\}$ NMR spectrum and one singlet in the ^{19}F NMR spectrum at -74.8 ppm. The corresponding signals due to the allyl substituents were observed in NMR spectra of compounds **10** – **12** with expected overall integral ratio to ArSb, i.e. 2:1 (ArSb), while for compound **13** the ratio is 1:1.

Molecular structures of compounds **10** – **13** were determined by X-ray analysis. Compounds **11** and **13** contain two structurally similar independent molecules in an elemental cell.

The molecular structures of compounds **10** – **12** are very similar and the Sb atom bridges two Pd atoms almost symmetrically (Figure 7). The bond angles Pd1–Sb–Pd2 are in the interval of 137.88(4) – 140.99(4)° and the angles C1–Sb1–Pd1 are in the range of 106.5(3) – 114.1(3)°. These values correspond to NBO analysis which proved that there is no electron lone pair on Sb atom, however, two analogous hybrid orbitals sp^2 are formed. Their overlap with hybrid orbitals of two Pd atoms leads to the formation of two Sb–Pd bonds. The bond lengths are in the range of 2.5585(5) – 2.6610(11) Å and very well correspond to a single bond [Σ_{cov}(Sb–Pd) = 2.60 Å] and are only slightly elongated when compared to compounds **6** [2.5363(6) Å] and **8** [2.541(4) Å]. In all studied compounds, the Sb atom is effectively coordinated by the pincer ligand and the bond lengths N→Sb indicate a strong intramolecular interaction with values in the narrow range of 2.360(2) – 2.432(2) Å, as was already the case with the above complexes. The N1–Sb–N2 bond angles range in interval 145.46(11) – 147.1(3)° which is in agreement to pseudo-meridional coordination of the pincer ligand.

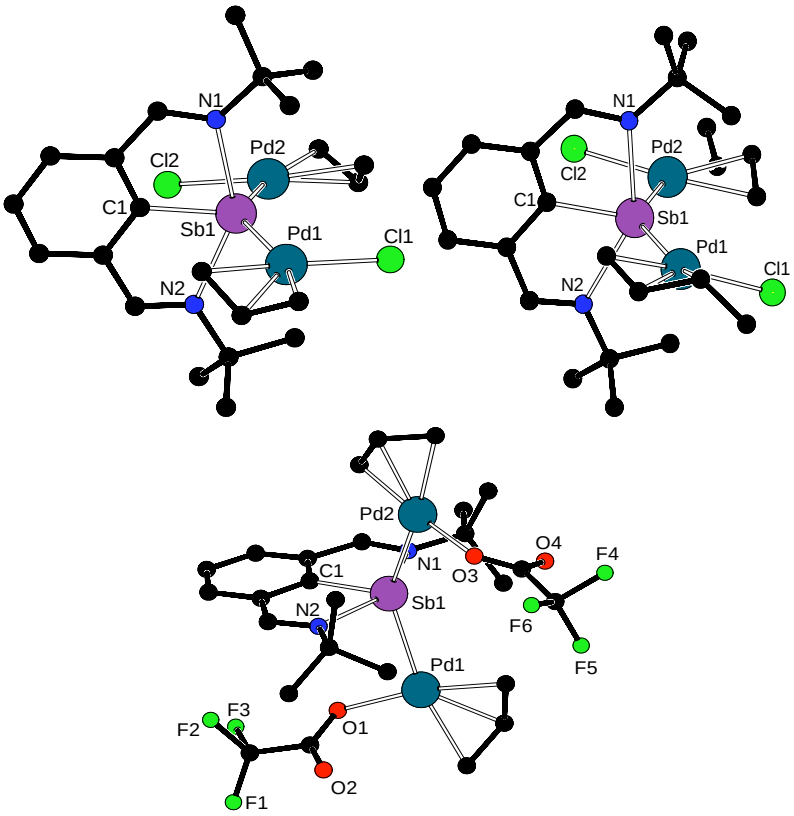

*Figure 7 Molecular structure of compounds **10** (top left), **11** (top right) and **12** (bottom).*

In contrast to these structures, only one Pd atom is coordinated to the Sb atom in compound **13**, and the Sb–Pd bond length is 2.5871(5) Å [2.5585(5) Å for the second independent molecule], which is comparable to compounds **10** – **12** (Figure 8). The value of the C1–Sb1–Pd1 bond angle of 104.66(14)° [110.22(15)° for the second independent molecule] corresponds to the side coordination of ArSb ligand, analogous to the previously prepared 1:1 complexes (Sb:TM). NBO analysis showed that Sb–Pd bond is formed by overlap of mainly *p*-orbital of Sb atom with hybrid orbital of Pd.

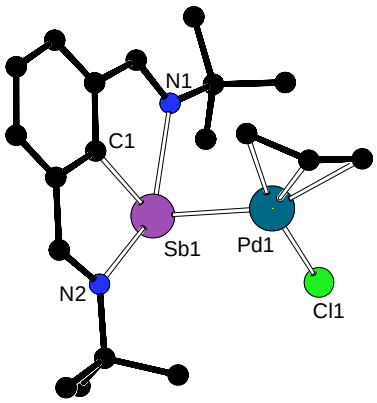

*Figure 8 Molecular structure of compound **13**.*

Group 11 complexes

Stibinidene ArSb was reacted with [AuCl(Me$_2$S)] in toluene at room temperature and after 20 minutes the precipitated complex [AuCl(ArSb)] (**14**) was isolated (Scheme 11). It can be stored in the solid state under an inert atmosphere at -30 °C for several weeks, but in a chloroform or dichloromethane solution it gradually decomposes to elemental gold and ArSbCl$_2$.

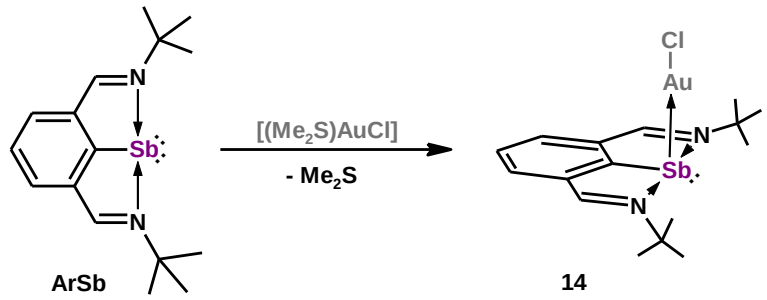

*Scheme 11 The synthesis of compound **14**.*

^{1}H a ^{13}C{^{1}H} NMR spectra in CDCl$_3$ contain the expected one set of signals for pincer ligand including *CH*=N groups with δ(^{1}H) = 8.92 ppm and δ(^{13}C) = 159.6 ppm.

To increase product stability, the reaction of stibinidene with tetrameric complex [Au(C≡CPh)]$_4$ was performed in benzene at room temperature to form the ion complex [Au(ArSb)$_2$]$^+$[Au(C≡CPh)$_2$]$^-$ (**15**) (Scheme 12). This complex exhibits better stability compared to compound **14** in the solid state, but again decomposes slowly in solution.

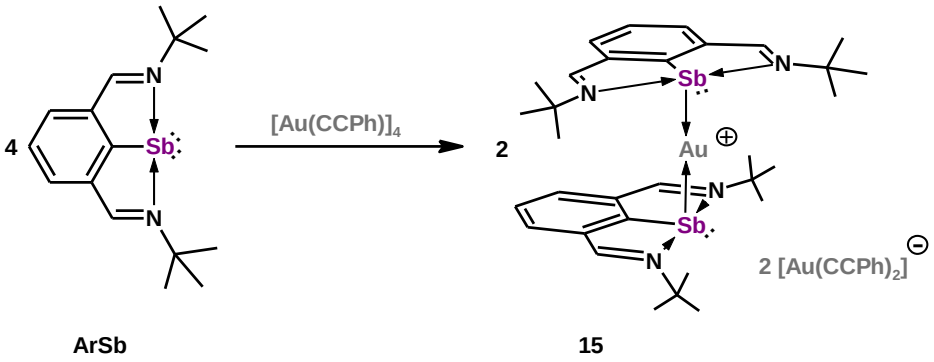

*Scheme 12 The synthesis of compound **15**.*

Analogously, one set of signals for *CH*=N groups with δ(^{1}H) = 9.00 ppm and δ(^{13}C) = 159.6 ppm can be observed in ^{1}H a ^{13}C{^{1}H} NMR spectra in CDCl$_3$. The aromatic region

of the spectra also contains the corresponding phenyl group signals in the expected integral ratio confirming the presence of the compensating anion $[Au(C{\equiv}CPh)_2]^-$.

Carbene ligands are known for their ability to stabilize a variety of gold complexes and have therefore been used in this study. Thus, the studied pnictinidenes were reacted with a gold complex $[Au(IPr)(MeCN)]^+[BF_4]^-$ [where IPr = 1,3-bis(2,6-diisopropylphenyl)-1,3-dihydro-2H-imidazol-2-ylidene] at room temperature in thf, which indeed yielded desired complexes $[Au(IPr)(ArE)]^+[BF_4]^-$, where E = Sb (**16**) and Bi (**17**) (Scheme 13). In this case, even a stable bismuthinidene complex was formed.

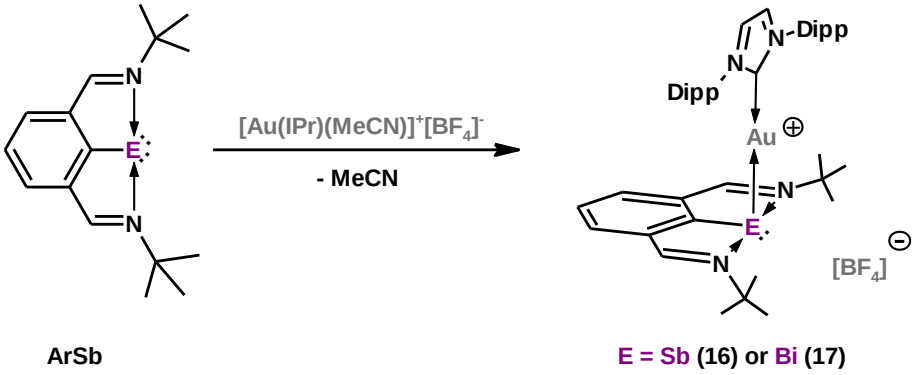

*Scheme 13 The synthesis of compounds **16** and **17**.*

Characterization of compounds **16** and **17** in solution was performed using ^1H a $^{13}C\{^1H\}$ NMR spectroscopy in thf-d_8. One set of signals for the pincer ligand was observed, including the signal for *CH*=N group with $\delta(^1H)$ = 9.13 and 9.51 ppm and $\delta(^{13}C)$ = 162.3 and 167.7 ppm for **16** and **17**. The presence of the carbene ligand could be confirmed by signals typical for Dipp groups in the corresponding integral ratio together with the IPr-*CH* group found at $\delta(^1H)$ = 7.53 and 7.56 ppm and $\delta(^{13}C)$ = 125.1 and 126.2 ppm. The $^{13}C\{^1H\}$ NMR spectra also contain a carbene carbon signal with $\delta(^{13}C)$ = 197.2 and 217.3 ppm.

The molecular structures of compounds **14** – **17** (Figure 9 – 11) were confirmed by X-ray analysis. All compounds show several common structural motives. The central pnictogen atom is tightly coordinated by the pincer ligand and the bond lengths N→E are 2.362(9) – 2.420(4) Å for E = Sb and 2.503(17) – 2.505(16) Å for E = Bi and show strong intramolecular interactions [Σ_{cov}(N–Sb) = 2.11 Å and Σ_{cov}(N–Bi) = 2.22 Å]. Values of the N1–E–N2 bond angles range from 141.7(5) to 155.6(3)°, which corresponds to the

pseudo-meridional fashion of ligand coordination. Side coordination of the ArE ligand is reflected by the C(*ipso*)–E–Au bond angles falling within a relatively narrow interval of 91.73(11) – 103.28(7)°, and hence the pnictogen is coordinated by utilization of *p*-type lone electron pair.

The Au–Sb bond length of 2.5204(5) Å in compound **14** (Figure 9) is comparable to the Σ_{cov}(Au–Sb) = 2.64 Å. The bond angle Cl1–Au1–Sb1 is 176.95(5)°.

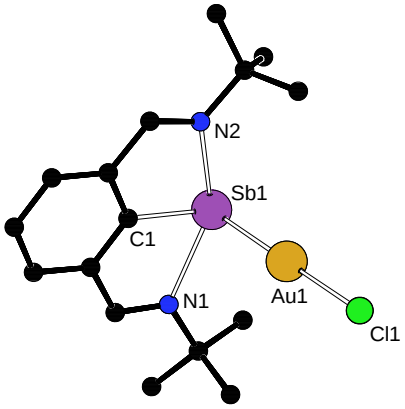

*Figure 9 Molecular structure of compound **14**.*

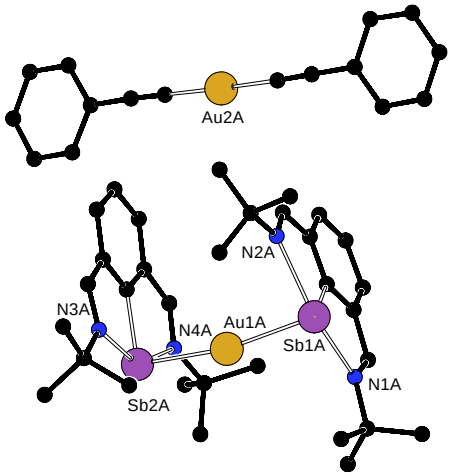

*Figure 10 Molecular structure of compound **15**.*

Compound **15** contains two independent molecules in unit cell and forms a well-separated ionic pair. In the structure of the cation (Figure 10), the central Au atom is coordinated by two Sb atoms with nearly linear geometry with an Sb1A–Au1A–Sb2A bond angle of 168.47(3)° [173.40(2)° for the second independent molecule]. Sb–Au bond lengths are found in the range of 2.5918(6) – 2.6027(6) Å and are longer than

those observed in compound **14** [2.5204(5) Å], which may be due to steric repulsion between two pincer ligands.

The structures of cations **16** and **17** (Figure 11), as expected, exhibit an almost linear central arrangement with C(carbene)–Au–E bond angles of 176.0(3) and 176.5(10)°. The bond lengths C(carbene)–Au are similar for both compounds, with a value of 2.051(11) Å for **16** and 2.03(2) Å for **17**. The bond length Sb–Au 2.5851(10) Å in cation **16** is longer than the value in complex **14** [2.5204(5) Å], but comparable to the values in cation **15** [2.5918(6) – 2.6027(6) Å]. The bond length of Bi–Au 2.659(11) Å in cation **17** is considerably shorter than Σ_{cov}(Au–Bi) = 2.75 Å. This differs significantly from the only compound with Bi(III)→Au(I) dative bond in the literature[9] where bond lenght Bi–Au is much longer (3,18 Å). The complex **17**, thus, is unique due to very strong interaction between those atoms. NBO anylsis showed that this Bi–Au σ-bond is implemented by donation from 6*p*-orbital of Bi to vacant 6*s*-orbital of Au.

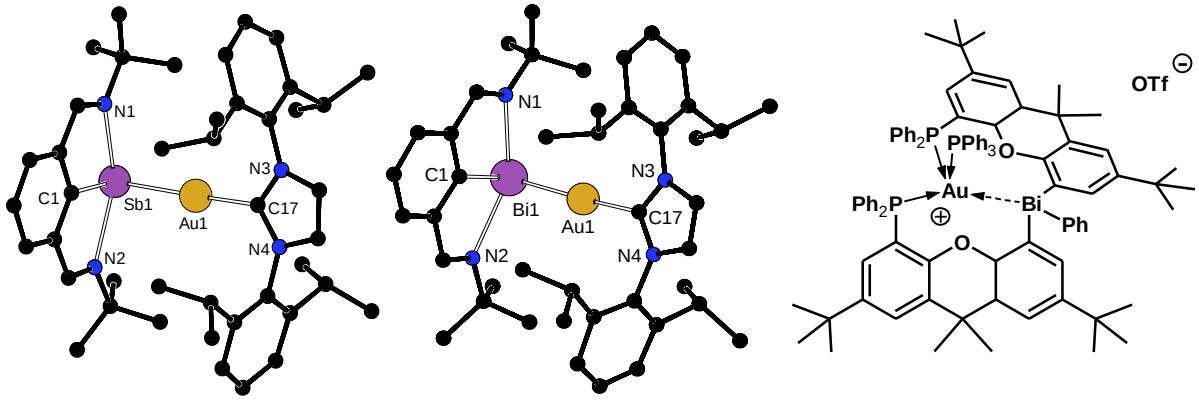

*Figure 11 Molecular structures of compounds **16** (left) and **17** (middle) and example of coumpound with Bi(III)→Au(I) dative bond (right).*

2.2. Pnictinidenes reactivity towards strong dienophiles

Reactions with substituted alkynes

Stibinidene ArSb reacts readily with electron deficient alkynes RC≡CR´ (R = CO_2Me, R´ = CO_2Me or H) in hexane at 0 °C and 1-stiba-1,4-dihydroiminonaphthalenes (**18** and **19**) are formed by cycloaddition (Scheme 14). However, compounds **18** and **19** show low stability in solution and decompose after only a few hours.

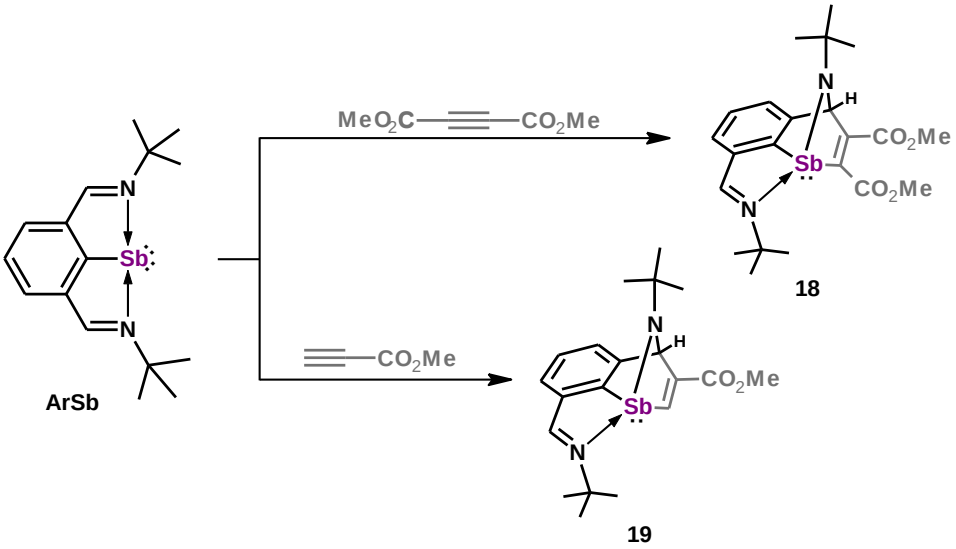

*Scheme 14 The synthesis of compounds **18** and **19**.*

The structure in solution was determined by ^{1}H a $^{13}C\{^{1}H\}$ NMR spectroscopy in C_6D_6. It was also confirmed that compound **19** is formed as a single regioisomer, i.e. the CH group of the unsymmetrical alkyne is bound to the antimony atom. The spectra of compounds **18** and **19** contain one set of signals for pincer ligand with typical chemical shift of the intact *CH*=N group with $\delta(^{1}H)$ = 7.97 and 8.04 ppm and $\delta(^{13}C)$ = 155.0 and 155.7 ppm. The second initially imine group involved in the reaction provides signals typical for the *CH*–N group found at $\delta(^{1}H)$ = 6.99 and 7.00 ppm and $\delta(^{13}C)$ = 81.4 and 78.9 ppm. The carbon atoms from the original C≡C alkyne bond provide two signals $\delta(^{13}C)$ = 159.1 and 162.9 ppm for **18**; 160.2 and 162.7 ppm for **19**. The ^{1}H-^{15}N HMBC spectra were also measured, where two signals with $\delta(^{15}N)$ = -32.1 and -32.4 ppm for the intact CH=*N* group and -237.6 and -244.6 ppm for the bridged CH–*N* group were observed.

The molecular structures of compounds **18** and **19** were confirmed by X-ray analysis (Figure 12). The central Sb atom is coordinated by three atoms and contains one lone electron pair. Thus, its geometry is close to the trigonal pyramid with the sum of the bond angles at Sb atom 243.3 or 243.0° (for compound **18** or **19**). The original Sb1–C1 bond length, which is also preserved in the products, corresponds to a single bond [2.1496(15) or 2.1316(15) Å]. In addition, two new covalent bonds were formed on the Sb atom, namely Sb1–C9 with a bond length of 2.1785(15) or 2.1775(17) Å and Sb1–N1 with a bond length of 2.0881(13) or 2.0902(15) Å. Both bonds correspond to the values for single bond [Σ_{cov}(Sb–N) = 2,11 Å and Σ_{cov}(Sb–C) = 2,15 Å]. In contrast, the bond length Sb1–N2 2.9970(13) or 2.9966(16) Å means that there is little interaction with the second donor group of ligand. Another newly formed single covalent bond is C7–C8 with length being 1.534(2) or 1.555(2) Å [Σ_{cov}(C–C) = 1.50 Å]. Due to double bonds C1–C2 [1.384(2) or 1.394(2) Å] and C9–C8 [1.335(2) or 1.336(2) Å], the central heterocycle with an annulated benzene ring is similar to 7-azabenzonorbornadiene.[10] It is noteworthy that compounds **18** and **19** are the first structurally characterized examples containing also second, heavier pnictogen in this structure.

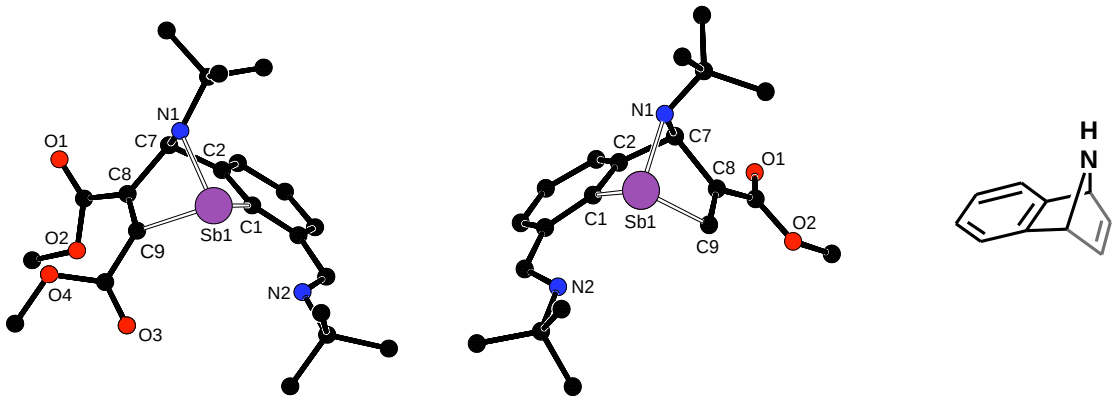

*Figure 12 Molecular structure of compounds **18** (left) and **19** (middle) and structure of 7-azabenzonorbornadiene (right).*

Reaction of bismuthinidene ArBi with symmetrically substituted alkyne DMAD in hexane at 0 ° C afforded compound **20** (Scheme 15). It is an analogue of compound **18**, but its stability in solution is substantially lower. However, the reaction with an unsymmetrically substituted alkyne RC≡CR´, where R/R´ = H/CO_2Me, gave different product. According to NMR spectroscopy, a mixture of compound **21** together with the starting bismuthinidene was obtained. Addition of another equivalent of alkyne resulted

in the quantitative formation of compound **21**. The same result can be obtained by reacting ArBi directly with two equivalents of the alkyne.

Characterization of both compounds in solution was performed using ^{1}H a $^{13}C\{^{1}H\}$ NMR spectroscopy in C_6D_6. The spectrum of compound **20** is analogous to that of **18**. For compounds **20** and **21**, signals were observed for one *CH*=N group with $\delta(^{1}H)$ = 8.03 or 8.32 ppm; $\delta(^{13}C)$ = 157.2 or 159.9 ppm and for the *CH*–N group found at $\delta(^{1}H)$ = 10.48 or 6.20 ppm; $\delta(^{13}C)$ = 92.9 or 67.7 ppm. The quaternary carbons of the parent alkyne linked by a double bond provide signals with $\delta(^{13}C)$ = 161.8 and 181.2 ppm for **20**; 145.5 and 179.5 ppm for **21**. Similarly, the $\delta(^{15}N)$ chemical shifts for CH=*N* group (-38.4 or -34.1 ppm) also correspond. Compound **20** contains a bridging CH–*N* group with $\delta(^{15}N)$ = -213.9 ppm, while in compound **21,** the amine *NH* group in ^{1}H-^{15}N HMBC is observed as doublet with $\delta(^{15}N)$ = -288.1 ppm ($^{1}J_{NH}$ = 69 Hz), and in the ^{1}H NMR spectrum as a characteristic singlet found at $\delta(^{1}H)$ = 0.80 ppm. The second alkyne in compound **21** with preserved triple bond provides signals with $\delta(^{13}C)$ = 100.1 and 111.1 ppm.

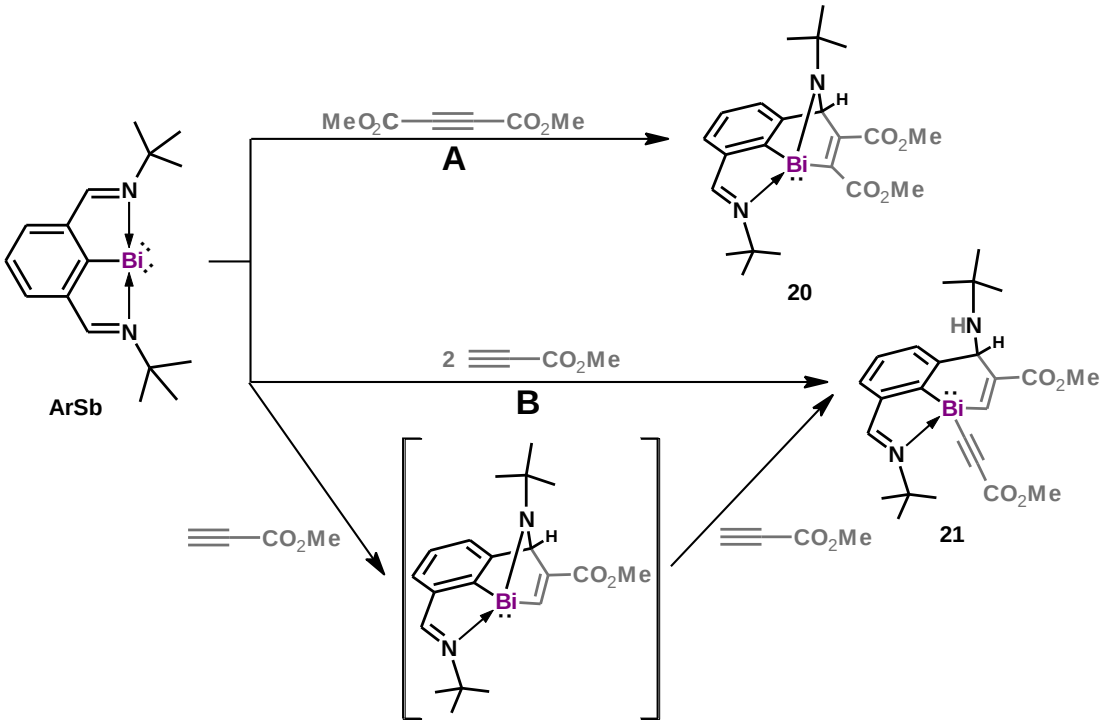

*Scheme 15 The synthesis of compounds **20** and **21**.*

The molecular structure of compound **21** was confirmed by X-ray (Figure 13). The central Bi atom is coordinated by three atoms and contains one lone electron pair.

Analogically to compounds **18** and **19**, the addition of one alkyne gives rise to novel covalent bonds Bi1–C11 with a bond length of 2.261(5) Å and C7–C8 with a bond length of 1.522(7) Å [Σ_{cov}(Bi–C) = 2.26 Å and Σ_{cov}(C–C) = 1.50 Å]. However, a second alkyne with Bi1–C16 bond length of 2.301(5) Å is also terminally bound to the Bi atom, while a triple bond is preserved between the C16 and C17 atoms with a length of 1.198(8) Å [Σ_{cov}(C≡C) = 1,20 Å]. Thus, the coordination polyhedron of the Bi atom corresponds to the trigonal pyramid, and the Bi1–N1 bond length of 2.811(4) Å can be described only as intramolecular interaction compared to compounds **18** and **19** [Σ_{cov}(Bi–N) = 2.22 Å]. Coordination of the second atom N2–Bi1 is even weaker [2.990(4) Å]. The central heterocycle can be described as bismacyclohexadiene with two bonds C1–C2 [1.383(9) Å] and C8–C11 [1.318(7) Å] which are corresponding to the double bond [Σ_{cov}(C=C) = 1.34 Å]. Similar structural fragments of phosphorus are known, but in the case of bismuth there is only one analogical example.[8]

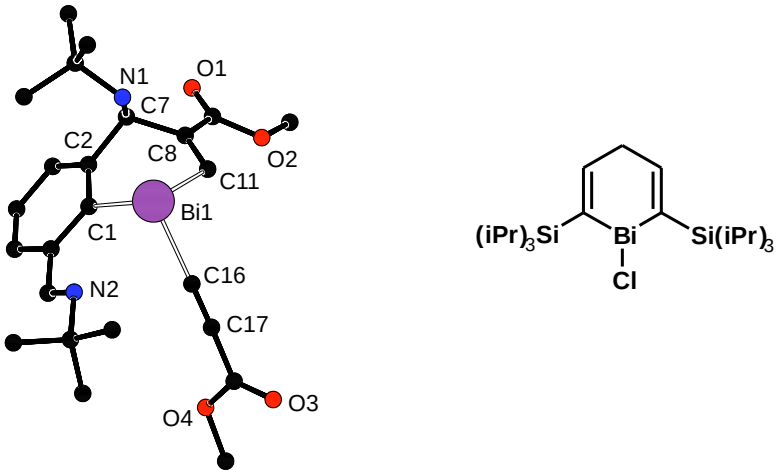

*Figure 13 Molecular structure of compound **21** (left) and example of analogical bismacyclohexadiene (right).*

Reaction with N-substituted maleimides

Based on the promising results mentioned above, a study of the reactivity of stibinidene with selected heterocycles containing a C=C multiple bond was also conducted. Thus, ArSb was reacted with *N*-substituted maleimides RN(C(O)CH)$_2$, where R = Me, tBu or Ph, in hexane at room temperature and the cycloaddition products **23** – **25** were formed within 5 minutes (Scheme 16).

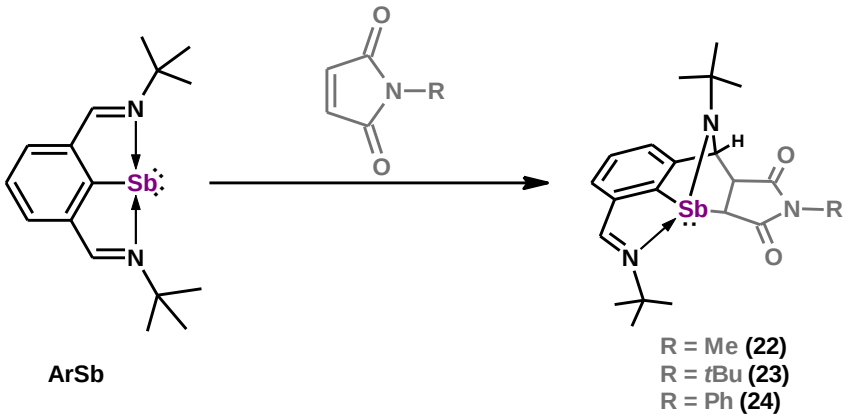

*Scheme 16 The synthesis of compounds **22** – **24**.*

The structure in solution was determined by ^{1}H, $^{13}C\{^{1}H\}$ and ^{15}N NMR spectroscopy in C_6D_6. The NMR spectra of all three compounds contain three sets of signals. The major set corresponds to the presence of the product, while the two minor sets indicate the presence of the starting compounds, i.e. stibinidene and the corresponding maleimide. Compounds **23** – **25** exhibit a typical *CH*=N signal with $\delta(^{1}H)$ = 7.99 – 8.00 ppm and $\delta(^{13}C)$ = 155.6 – 155.7 ppm. Compared to this group, the chemical shifts of the newly formed *CH*–N group found at $\delta(^{1}H)$ = 6.24 – 6.37 ppm and $\delta(^{13}C)$ = 75.3 – 76.2 ppm are significantly shifted (i.e. the X signal from the ABX spin system, Figure 14). The signals for the two *CH* groups of the maleimide moiety are part of the above mentioned ABX spin system with $\delta(^{1}H)$ = 2.21 – 2.42 and 2.36 – 2.56 ppm (i.e. signal B and A) and chemical shifts $\delta(^{13}C)$ are in the range of 42.6 – 49.8 ppm. Thus, they are significantly shifted compared to the CH=CH bond of the starting maleimides [$\delta(^{1}H)$ = 5.65 – 5.73 ppm and $\delta(^{13}C)$ = 133.7 ppm]. Three signals can be observed in ^{1}H-^{15}N HMBC spectra, for CH=*N* group [$\delta(^{15}N)$ = -30.9 – -37.2 ppm], CH–*N* group [$\delta(^{15}N)$ = -271.2 – -277.9 ppm] and *N*-imide [$\delta(^{15}N)$ = -190.3 – -209.9 ppm].

The dynamic equilibrium between the two starting materials and the corresponding product in solution was demonstrated by the addition of an excess of ArSb, which led to the equilibrium shift in favor of the products and a complete disappearance of the NMR signals for the corresponding maleimide. Analogously, this demonstration was also done by adding an excess of maleimide (Figure 14, B and C). This phenomenon was also confirmed by ^{1}H-^{1}H EXSY spectroscopy. For example, for compound **22**, chemical exchange can be observed between Me group of the product

[δ(¹H) = 2.82 ppm] and starting maleimide [δ(¹H) = 2.49 ppm], or between the CH=N group of the product [δ(¹H) = 8.02 ppm] and starting stibinidine [δ(¹H) = 8.91 ppm] (Figure 14, EXSY arrows between Me and Me; CH=N and CH=N). This suggests that compounds **23** – **25** decompose back to the starting materials in the solution and, thus, the addition of the CH=CH bond of maleimide is reversible.

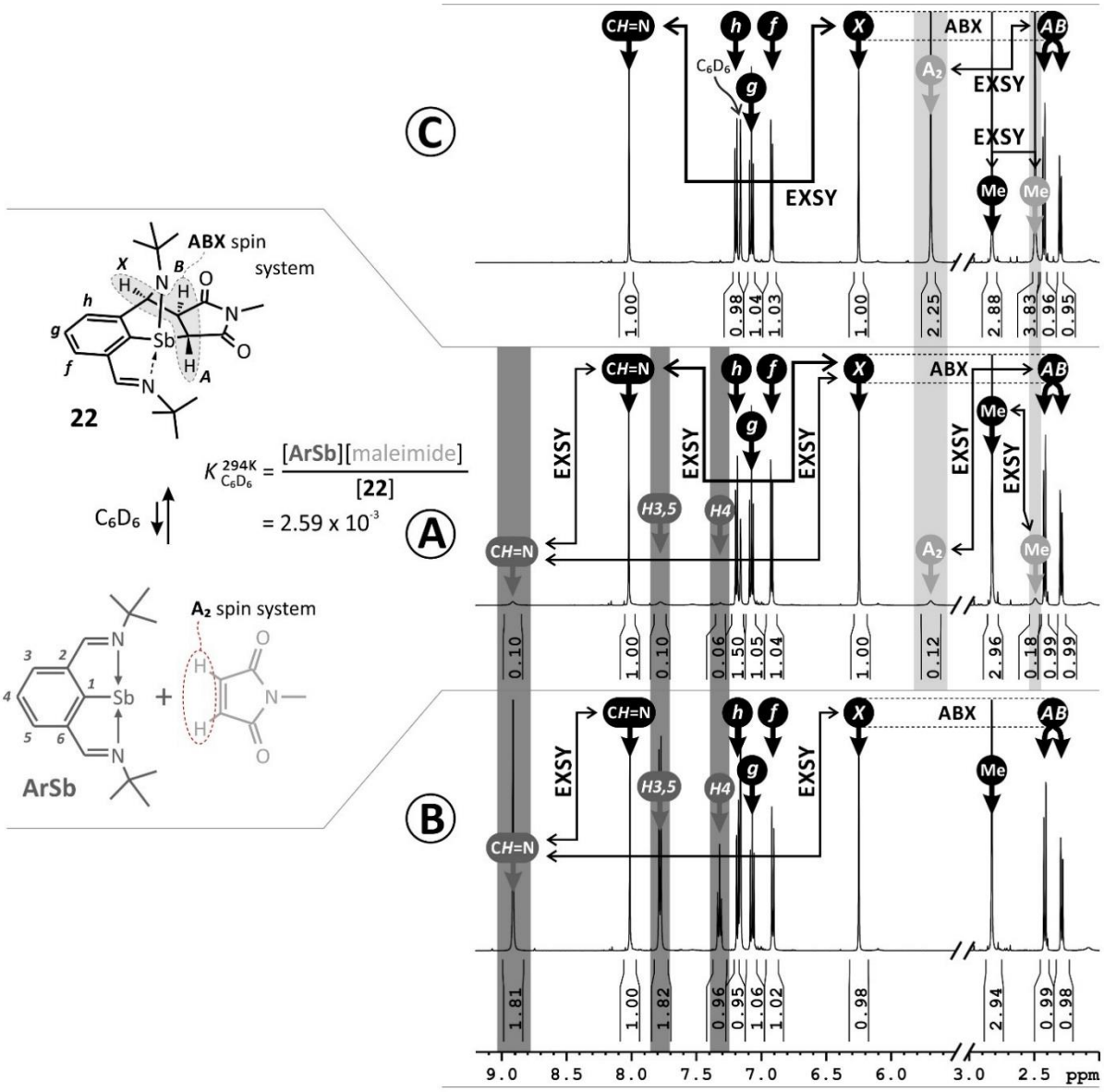

*Figure 14 Stacked plot of ¹H NMR spectra (500.20 MHz, C_6D_6, 294 K). Dissolved single-crystals of **22** (A), dissolved single-crystals of **22** with added excess of ArSb (B) and dissolved single-crystals of **22** with added excess of N-methylmaleimide (C).*

For this reason, all compounds were also studied by ^{1}H VT-NMR spectroscopy (Figure 15). By increasing the temperature of the toluene solutions of compounds **23** – **25**, the equilibrium is shifted in favor of the starting materials. Reversibility of this process has been demonstrated by repeated heating and cooling of the samples. Based on the temperature dependence of the equilibrium constant *K*, the thermodynamic parameters for the reaction in toluene-d_8 were calculated with the following values: ΔG° = -3.48 kcal·mol^{-1}; ΔH° = -16.51 kcal·mol^{-1}; ΔS° = -43.72 cal·K^{-1}·mol^{-1} (**23**); ΔG° = -1.94 kcal·mol^{-1}; ΔH° = -16.39 kcal·mol^{-1}; ΔS° = -48.48 cal·K^{-1}·mol^{-1} (**24**); ΔG° = -2.59 kcal·mol^{-1}; ΔH° = -16.56 kcal·mol^{-1}; ΔS° = -46.87 cal·K^{-1}·mol^{-1} (**25**).

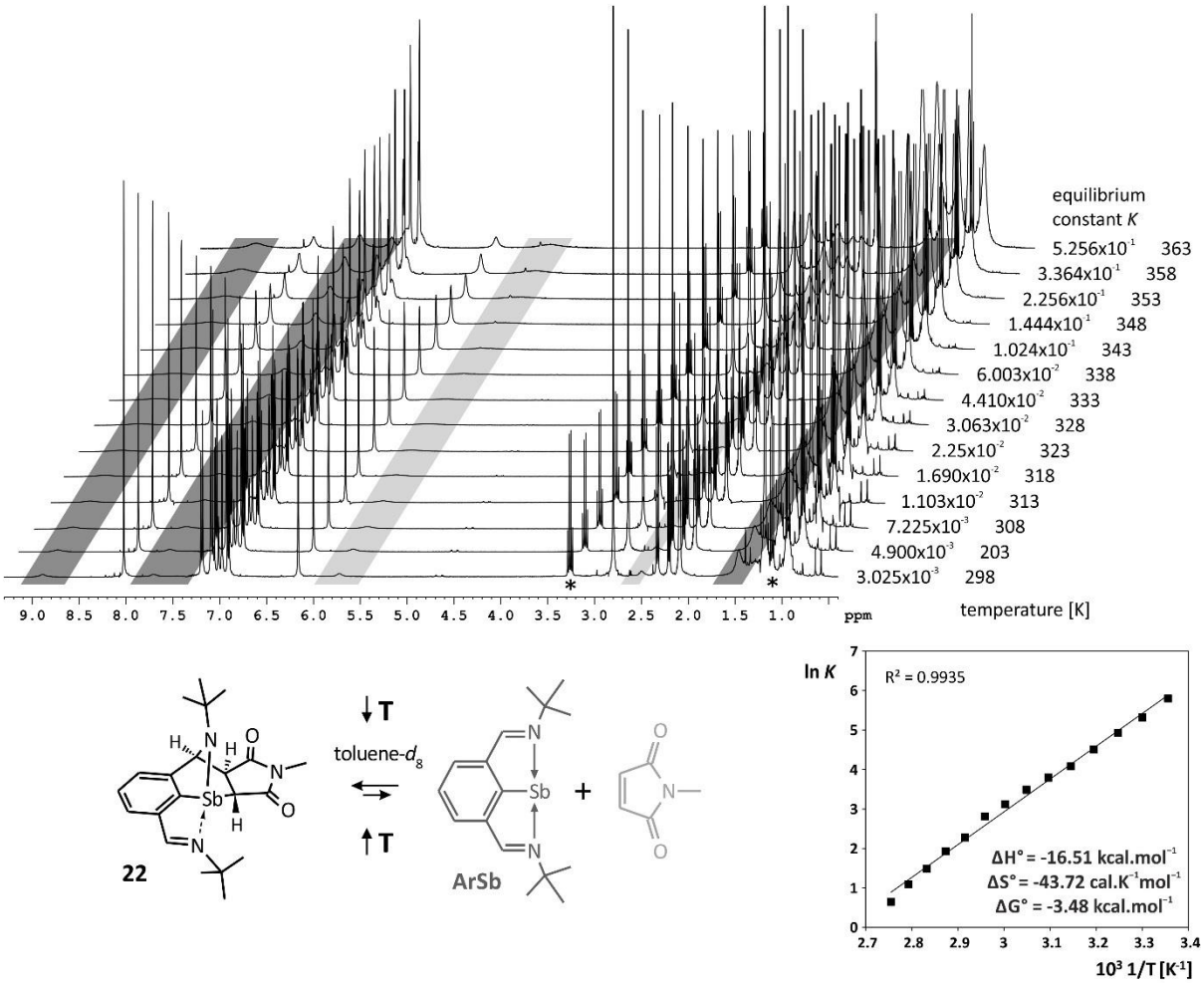

*Figure 15 Stacked plot of ^{1}H VT-NMR spectroscopy (400.13 MHz, toluene-d_8) of compound **22** and van't Hoff plot. * indicates the Et_2O traces.*

The molecular structures of compounds **23** – **25** were confirmed by X-ray analysis (Figure 16). The central Sb atom has the geometry of trigonal pyramid due to the formation of Sb1–C17 bonds with a length in the interval of 2.199(3) – 2.211(3) Å

corresponding to the Σ_{cov}(Sb–C) = 2.15 Å, and Sb1–N1 with a bond length in the interval of 2.082(2) – 2.090(7) Å, which corresponds very well to the covalent bond [Σ_{cov}(Sb–N) = 2.11 Å]. In contrast, the second N2 atom remains only weakly intramolecularly coordinated [2.9405(18) – 2.962(3) Å]. Another newly formed C7–C20 covalent bond has lengths of 1.564(4) – 1.565(5) Å corresponding to a single bond [Σ_{cov}(C–C) = 1.50 Å], whereas the C7 atom originally from the CH=N group shows tetrahedral geometry. Originally multiple bond between C17 and C20 exhibits bond lengths of 1.528(5) – 1.535(12) Å, which corresponds to a single bond.

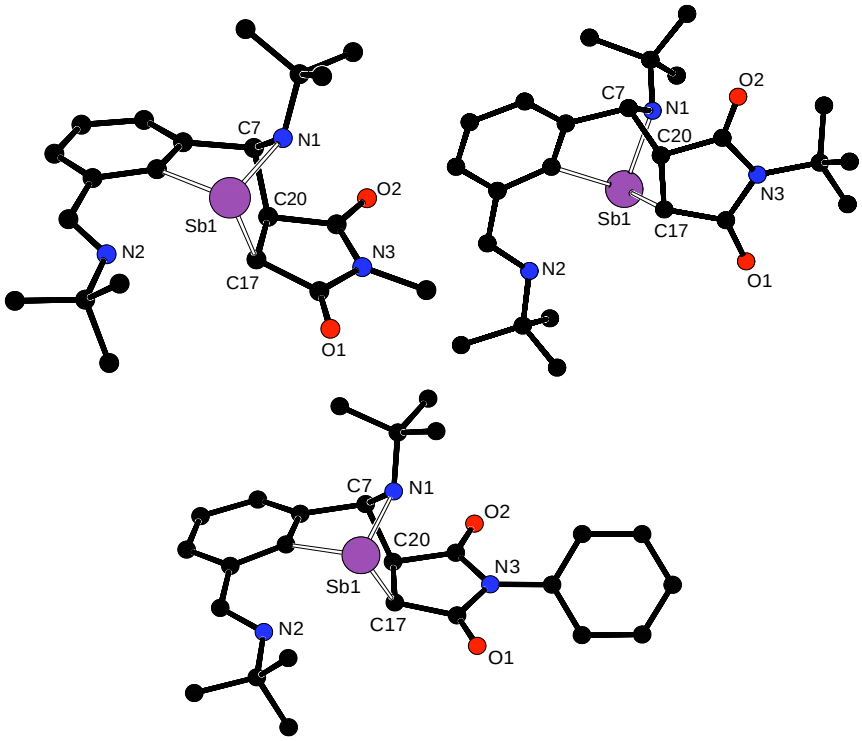

*Figure 16 Molecular structure of compounds **22** (top left), **23** (top right) and **24** (bottom).*

3. SUMMARY

The chemistry of the heavier pnictinidines is not very well known and therefore not enough attention has been paid to their reactivity. In terms of the electron structure of these compounds, the pnictinidenes can be regarded primarily as compounds containing two lone electron pairs at the central atom of Group 15. Based on previous works,[3] the study focused on their coordination possibilities, i.e. their use as ligands in the chemistry of other TMs and even with non-carbonyl complexes, and the attention was focused on the potential use of both electron pairs for coordination. As noted, the lighter *(N)CN* chelated pnictinidenes may also exhibit diene or aromatic behavior. For this reason, reactivity to strong dienophiles was studied in this work too.

The common feature of all prepared 1:1 complexes (E:TM) of Group 9 – 11 is the possibility of bond formation between E and TM. It was found out that just a *p*-type pair of the two lone electron pairs on pnictogen is used for *σ*-bond, while the *s*-type pair remains inert (see the scheme below, reaction A). Thus, the TM is coordinated almost perpendicularly to the plane of the ArSb or ArBi ligand. At the same time, it was also confirmed that *NCN* chelated stibinidene can indeed act as four-electron donor with allylpalladium complexes (reaction B). It was corroborated by NBO analysis that two sp^2 hybrid orbitals on Sb atom are formed.

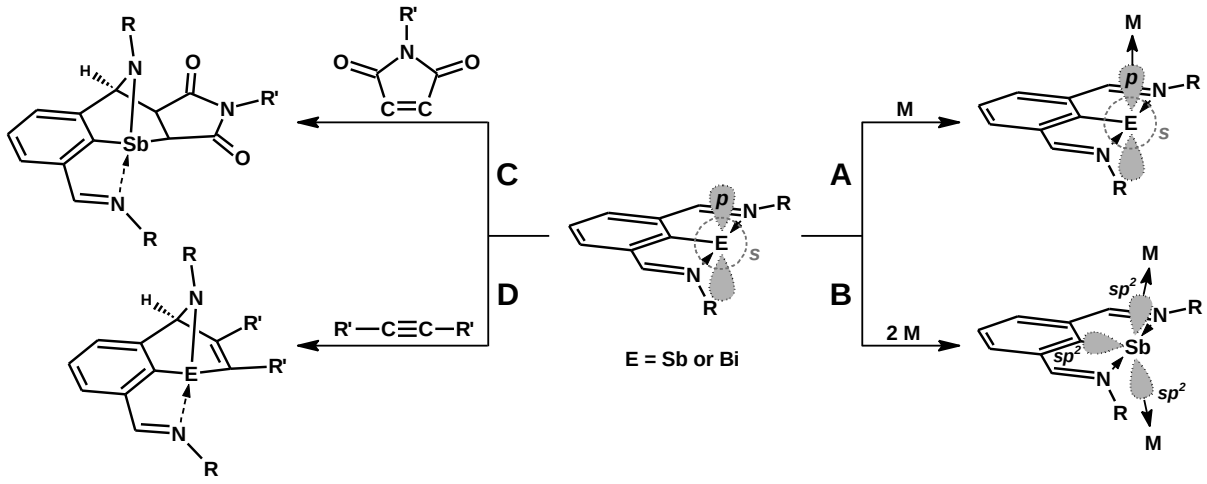

The second part of this work was devoted to reactions of pnictinidenes with selected organic substrates containing C–C multiple bonds to experimentally prove their potential to participate as heterodienes in Diels-Alder reaction. It has been shown that, as expected, they indeed lead to cycloaddition reaction producing unique heterocyclic

compounds, thereby confirming the considered diene character of the heavier *NCN* chelated pnictinidenes as well (reaction C, D). Importantly, it has been also shown that the reaction with *N*-substituted maleimides is completely reversible and, therefore, very important in terms of possible catalysis utilization.

4. REFERENCES

1. a) L. Liu, D. A. Ruiz, D. Munz, G. Bertrand, *Chem 1*, **2016**, 147. b) J. Hyvl, W. Y. Yoshida, A. L. Rheingold, R. P. Hughes, M. F. Cain, *Chem. Eur. J*., **2016**, *22*, 17562. c) S. Shah, J. D. Protasiewicz, *Chem. Commun*., **1998**, 1585. d) A. J. Arduengo, J. C. Calabrese, A. H. Cowley, H. V. Rasika Dias, J. R. Goerlich, W. J. Marshall, B. Riegel, *Inorg. Chem*., **1997**, *36*, 2151.

2. a) L. M. Opris, A. Silvestru, C. Silvestru, H. J. Breunig, E. Lork, *Dalton Trans.*, **2004**, 3575. b) H. J. Breunig, L. Balazs, *Organometallics*, **2004**, *23*, 304. c) R. Waterman, T. D. Tilley, *Angew. Chem., Int. Ed.*, **2006**, *45*, 2926. d) G. Huttner, K. Evertz, *Acc. Chem. Res.*, **1986**, *19*, 406.

3. a) I. Vránová, V. Kremláček, M. Erben, J. Turek, R. Jambor, A. Růžička, M. Alonso, L. Dostál, *Dalton Trans.*, **2017**, *46*, 3556. b) I. Vránová, M. Alonso, R. Jambor, A. Růžička, M. Erben, L. Dostál, *Chem. Eur. J.*, **2016**, *22*, 7376.

4. a) L. M. Opris, A. Silvestru, C. Silvestru, H. J. Breunig, E. Lork, *Dalton Trans.*, **2004**, 3575. b) L. Balázs, H. J. Breunig, E. Lork, C. Silvestru, *Eur. J. Inorg. Chem.*, **2003**, 1361.

5. I. Vránová, T. Dušková, M. Erben, R. Jambor, A. Růžička, L. Dostál, *J. Organomet. Chem.*, **2018**, *863*, 15.

6. a) J. Hyvl, W. Y. Yoshida, A. L. Rheingold, R. P. Hughes, M. F. Cain, *Chem. Eur. J.*, **2016**, *22*, 17562. b) V. Kremláček, J. Hyvl, W. Y. Yoshida, A. Růžička, A. L. Rheingold, J. Turek, R. P. Hughes, L. Dostál, M. F. Cain, *Organometallics*, **2018**, *37*, 2481.

7. a) D. G. Hall, T. Rybak, T. Verdelet, *Acc. Chem. Res.*, **2016**, *49*, 2489. b) J. J. Zhao, S. B. Sun, S. H. He, Q. Wu, F. Shi, *Angew. Chem.*, **2015**, *127*, 5550.

8. T. Ishii, K. Suzuki, T. Nakamura, M. Yamashita, *J. Am. Chem. Soc.*, **2016**, *138*, 12787.

9. K. Materne, S. Hoof, N. Frank, C. Herwig, C. Limberg, *Organometallics*, **2017**, *36*, 4891.

10. L. A. Carpino, D. E. Barr, *J. Org. Chem.*, **1966**, *31*, 764.

5. LIST OF PAPERS PUBLISHED BY THE AUTHOR

Papers in the topic of the thesis:

1. *Reactions of N,C,N-chelated pnictinidenes with Rh(I) and Ir(I) complexes: Coordination vs. Transmetalation*; M. Kořenková, V. Kremláček, M. Erben, R. Jambor, Z. Růžičková, L. Dostál, *J. Organomet. Chem.*, **2017**, *845*, 49. **DOI: 10.1016/j.jorganchem.2017.02.022**

2. *Synthesis and non-conventional structure of square-planar Pd(II) and Pt(II) complexes with an N,C,N-chelated stibinidene ligand*; M. Kořenková, M. Hejda, P. Štěpnička, F. Uhlík, R. Jambor, A. Růžička, L. Dostál, *Dalton Trans.*, **2018**, *47*, 5812. **DOI: 10.1039/c8dt00714d**

3. *Antimony(I) → Pd(II) complexes with the (μ-Sb)Pd_2 coordination framework*; M. Kořenková, M. Hejda, R. Jirásko, T. Block, F. Uhlík, R. Jambor, A. Růžička, R. Pöttgen, L. Dostál, *Dalton Trans.*, **2019**, *48*, 11912. **DOI: 10.1039/c9dt02340b**

4. *Heavier pnictinidene gold(I) complexes*; M. Kořenková, V. Kremláček, M. Erben, R. Jirásko, F. De Proft, J. Turek, R. Jambor, A. Růžička, I. Císařová, L. Dostál, *Dalton Trans.*, **2018**, *47*, 14503. **DOI: 10.1039/c8dt03022g**

5. *Hetero Diels-Alder Reactions of Masked Dienes Containing Heavy Group 15 Elements;* M. Kořenková, V. Kremláček, M. Hejda, J. Turek, R. Khudaverdyan, M. Erben, R. Jambor, A. Růžička, L. Dostál, *Chem. Eur. J.*, **2020**, *26*, 1144. ***DOI: 10.1002/chem.201904953***

6. *Reversible C=C Bond Activation by an Intramolecularly Coordinated Antimony(I) Compound*; M. Kořenková, M. Hejda, M. Erben, R. Jirásko, R. Jambor, A. Růžička, E. Rychagova, S. Ketkov, L. Dostál, *Chem. Eur. J.*, **2019**, *25*, 12884. **DOI: 10.1002/chem.201902968**

Papers out of the topic of the thesis:

7. *Different hydrolytic stabilities of some C,N-chelated germanium alkoxides*; M. Kořenková, R. Jambor, Z. Růžičková, L. Dostál, Inorg. Chem. Commun., **2016**, *69*, 28. **DOI: 10.1016/j.inoche.2016.04.020**

8. *The reactivity of N,C,N-intramolecularly coordinated antimony(III) and bismuth(III) oxides with the sterically encumbered organoboronic acid 2,6-i-$Pr_2C_6H_3B(OH)_2$;* M. Kořenková, M. Erben, R. Jambor, A. Růžička, L. Dostál*, J. Organomet. Chem.,* **2014***, 772 - 773,* 287. **DOI: 10.1016/j.jorganchem.2014.09.032**

9. *Synthesis of heteroboroxines with MB_2O_3 core (M = Sb, Bi, Sn)—an influence of the substitution of parent boronic acids; M.* Kořenková, B. Mairychová, A. Růžička, R. Jambor, L. Dostál, *Dalton Trans.*, **2014**, *43*, 7096. **DOI: 10.1039/c3dt53012d**

10. *Opening of boroxines by N,C,N-chelated antimony(III), bismuth(III) and tin(IV) compounds;* M. Kořenková, B. Mairychová, R. Jambor, Z. Růžičková, L. Dostál, *Inorg. Chem. Commun.*, **2014**, *47*, 128. **DOI: 10.1016/j.inoche.2014.07.028**